Cedarville University

DigitalCommons@Cedarville

Pharmaceutical Sciences Faculty Publications

Department of Pharmaceutical Sciences

6-1-2012

A Humanized Pattern of Aromatase Expression is Associated with Mammary Hyperplasia in Mice

Hong Zhao

Elizabeth K. Pearson

David C. Brooks

John S. Coon

Dong Chen

See next page for additional authors

Follow this and additional works at: https://digitalcommons.cedarville.edu/pharmaceutical_sciences_publications

Part of the Pharmacy and Pharmaceutical Sciences Commons

CENTENNIAL LIBRARY
CEDARVILLE UNIVERSITY

Authors

Hong Zhao, Elizabeth K. Pearson, David C. Brooks, John S. Coon, Dong Chen, Masashi Demura, Ming Zhang, Charles V. Clevenger, Xia Xu, Timothy D. Veenstra, Robert T. Chatterton, Francesco J. DeMayo, and Serdar E. Bulun

A Humanized Pattern of Aromatase Expression Is Associated with Mammary Hyperplasia in Mice

Hong Zhao, Elizabeth K. Pearson, David C. Brooks, John S. Coon V, Dong Chen,
Masashi Demura, Ming Zhang, Charles V. Clevenger, Xia Xu,
Timothy D. Veenstra, Robert T. Chatterton, Francesco J. DeMayo, and
Serdar E. Bulun

Division of Reproductive Biology Research, Departments of Obstetrics and Gynecology (H.Z., E.K.P., D.C.B., J.S.C., D.C., M.D., R.T.C., S.E.B.), Medicine (M.Z.), Pathology (C.V.C.), and Physiology (R.T.C.), Feinberg School of Medicine, Northwestern University, Chicago, Illinois 60611; Laboratory of Proteomics and Analytical Technologies (X.X.,T.D.V.), Science Applications International Corporation-Frederick, National Cancer Institute, National Institutes of Health, Frederick, Maryland 21702; and Department of Molecular and Cellular Biology (F.J.D.), Baylor College of Medicine, Houston, Texas 77030

Aromatase is essential for estrogen production and is the target of aromatase inhibitors, the most effective endocrine treatment for postmenopausal breast cancer. Peripheral tissues in women, including the breast, express aromatase via alternative promoters. Female mice lack the promoters that drive aromatase expression in peripheral tissues; thus, we generated a transgenic humanized aromatase (Arom[hum]) mouse line containing a single copy of the human aromatase gene to study the link between aromatase expression in mammary adipose tissue and breast pathology. Arom[hum] mice expressed human aromatase, driven by the proximal human promoters II and I.3 and the distal promoter I.4, in breast adipose fibroblasts and myoepithelial cells. Estrogen levels in the breast tissue of Arom[hum] mice were higher than in wild-type mice, whereas circulating levels were similar. Arom[hum] mice exhibited accelerated mammary duct elongation at puberty and an increased incidence of lobuloalveolar breast hyperplasia associated with increased signal transducer and activator of transcription-5 phosphorylation at 24 and 64 wk. Hyperplastic epithelial cells showed remarkably increased proliferative activity. Thus, we demonstrated that the human aromatase gene can be expressed via its native promoters in a wide variety of mouse tissues and in a distribution pattern nearly identical to that of humans. Locally increased tissue levels, but not circulating levels, of estrogen appeared to exert hyperplastic effects on the mammary gland. This novel mouse model will be valuable for developing tissue-specific aromatase inhibition strategies. (**Endocrinology** 153: 2701–2713, 2012)

Aromatase, encoded by a single gene, is essential for estrogen production. Estrogens exert their effects by binding to two distinct receptors, estrogen receptor (ER)-α and ERβ (1, 2). Aromatase and epithelial ERα expression are required for normal mammary gland development involving ductal elongation and outgrowth during puberty (3, 4). Aromatase and estrogen are also involved in the development of hormone-dependent breast cancer, and aromatase inhibitors are the most effective endocrine treatment for postmenopausal breast cancer (5, 6). The causal relationship between estrogen and breast cancer has been well documented in studies of several breast cancer cell lines (7). Ligand-activated ER acts in the nucleus as a transcriptional factor or interacts with and activates cytoplasmic signaling molecules including c-Src, signal transducer and activator of transcription (Stat), ERK, and phosphatidylinositol 3-kinase (PI3K)/ Akt (8, 9).

Abbreviations: Arom[hum], Transgenic humanized aromatase; BCA, bicinchoninic acid protein assay; E_1, estrone; E_2, estradiol; E_3, estriol; ER, estrogen receptor; GAPDH, glyceraldehyde-3-phosphate dehydrogenase; HCG, human chorionic gonadotropin; LC-MS[2], liquid chromatography-tandem mass spectrometry; 2ME$_1$, 2-methoxyestrone; 2ME$_2$, 2-methoxyestradiol; PI3K, phosphatidylinositol 3-kinase; PMSG, pregnant mares' serum gonadotropin; PR, progesterone receptor; RACE, rapid amplification of cDNA ends; Stat, signal transducer and activator of transcription; WT, wild type.

Both human and mouse aromatase genes comprise 10 exons, nine of which are coding exons (II-X) that span approximately 30 kb. A number of alternative noncoding first exons are expressed in a tissue-specific manner and are spliced onto a common junction upstream of the translation start site, resulting in the synthesis of identical aromatase proteins regardless of the first exon used (5, 10). In humans, 10 alternative tissue-specific first exons have been identified in various tissues: exons I.1, I.2, and I.2a in placenta (−93, −78, and −13 kb); I.4 in adipose tissue and skin (−73 kb); I.5 in fetal tissues (−43 kb); I.7 in endothelial cells (−36 kb); I.f in brain (−33 kb); I.6 in bone (−1kb); I.3 in breast fat proximal to cancer (−0.3 kb); and PII in gonads (−0.1 kb) (11). In contrast to the human gene, there are only two tissue-specific untranslated first exons in the female mouse aromatase gene: a gonadal-specific exon (−0.1 kb) and a brain-specific exon (−35.5 kb) (12–14). Compared with mice, then, women express aromatase via alternatively used promoters in a number of additional peripheral tissues (*e.g.* breast adipose), giving rise to drastically distinct tissue distribution patterns of aromatase expression.

Thus far, two transgenic mouse lines expressing human aromatase have been reported: mice expressing human aromatase driven by the mouse mammary tumor virus-long-terminal repeat promoter (int-5/aromatase) and mice expressing human aromatase driven by the human ubiquitin C promoter (15). Int-5/aromatase female mice exhibit mammary duct hyperplasia, ductal dysplastic lesions, alveolar hyperproliferation, and fibroadenomas (16). The phenotype of the mice expressing human aromatase driven by the human ubiquitin C promoter is characterized by mammary hyperplasia in 15-month-old females (15, 17). Although these two animal models have helped in understanding the molecular mechanisms involved in the formation of the mammary glands and the development of breast cancer, they do not mimic human aromatase expression patterns in peripheral tissues driven by native promoters; therefore, they are not ideal models for developing tissue-specific aromatase inhibition strategies (12, 18).

In premenopausal women, the ovaries express high levels of aromatase and are the main source of estrogens. However, extragonadal aromatase expression plays a key role in estrogen production, especially in men and postmenopausal women, because ovarian aromatase expression ceases after menopause (11). Estrogens synthesized locally in extragonadal sites do not typically enter the circulation; rather, local estrogens exert intracrine, autocrine, paracrine, and juxtacrine effects, acting directly on cells and tissues. These effects are very difficult to measure in the clinical setting, and they remain mostly unrecognized.

We and others have proposed that adipose tissue aromatase is the major determinant of local levels of estrogen in the breast and is linked to breast cancer risk (19, 20). Because female mice lack the promoters for aromatase expression in extragonadal tissues, such as the breast adipose, we generated a transgenic humanized aromatase (Arom^{hum}) mouse line that contains a single copy of the human aromatase gene and mimics human physiology with respect to tissue-specific patterns of aromatase expression and estrogen production. Here we report the molecular and functional aspects of humanized aromatase expression in the mammary gland and other peripheral tissues in the Arom^{hum} mice and the potential application for the study of the relationship between breast aromatase expression, estrogen production, obesity, and breast cancer pathology.

Materials and Methods

Bacterial artificial chromosome (BAC) clones characterization and generation of transgenic mice

Three BAC clones were obtained from the BACPAC Resources Center of Children's Hospital Oakland Research Institute (Oakland, CA). BAC DNA was transformed into competent bacteria (DH10B) and grown in Luria-Bertani medium containing 12.5 μg/ml chloramphenicol. BAC DNA was extracted by the alkaline lysis method. The sizes of the BAC were estimated by *Not*I linearized restriction digestion and 0.6% agarose gel electrophoresis. The ends of the BAC were sequenced, and a large-scale *Eco*RV restriction map was generated (data not shown). Aromatase gene integrity was confirmed with PCR primer pairs that hybridize to its promoter regions (I.1, I.4, I.7, I.f, I.6, I.3, and PII) and coding region (exon II and exon X; data not shown) (21, 22). One of the BAC clones (RP11–1134K1) contained the complete aromatase locus and was subsequently used for all studies. Linearized RP11-1134K1 DNA was microinjected into the pronucleus of strain FVB/N-fertilized oocytes at the Baylor College of Medicine Genetically Engineered Mouse Core (Houston, TX). Integration of the transgene in the offspring was assessed by PCR analysis. The primer sequences used for screening PCR are listed in Supplemental Table 1, published on The Endocrine Society's Journals Online web site at http://endo.endojournals.org.

Genotyping and animals

Genotypic analyses were performed by PCR using genomic DNA isolated from the tails of potential founder mice. Initial genotyping was done using the PCR primers described above. Similar phenotypes of mammary hyperplasia were observed in two independent transgenic lines, F1771 and F1772. Both lines contained the complete human aromatase coding region. The F1771 line contained a longer promoter region, starting 75 kb upstream of the ATG translation start site and including promoters I.4, I.7, I.f, I.6, I.3, and PII. The F1772 line contained a shorter promoter region, starting 4.3 kb upstream of the trans-

lation start site and including promoters I.6, I.3, and PII. Mice were maintained on a 14-h light, 10-h dark cycle, with standard chow (7912; Harlan Teklad, Madison, WI) and water available *ad libitum*. Animals were housed according to the National Institutes of Health Guide for the Care and Use of Laboratory Animals. All procedures were approved by the Animal Care and Use Committees of Baylor College of Medicine and Northwestern University. All tissues and serum were collected from mice between 1000 and 1200 h to remove variability in daily hormone fluctuations.

RNA isolation and quantitative real-time PCR

Total RNA from various mouse tissues was extracted at 24 and 64 wk of age using TRIzol reagent according to the manufacturer's instructions (Sigma, St. Louis, MO). cDNA was reverse transcribed using oligo(deoxythymidine) primers and a reverse transcriptase kit (Invitrogen Corp., Carlsbad, CA). Real-time PCR was performed with the Taqman and Power SYBR® green PCR master mix kit according to the manufacturer's instructions (Applied Biosystems, Foster City, CA) in an ABI 7900HT fast real-time PCR system (Applied Biosystems). The primer sequences used for real-time PCR are listed in Supplemental Table 1. Real-time PCR cycler conditions were: 50 C for 2 min, 95 C for 10 min, and 40 cycles of 95 C for 15 sec and 60 C for 1 min. PCR results were normalized to mouse glyceraldehyde-3-phosphate dehydrogenase (*GAPDH*) gene expression (23). Cycle threshold values at or above 40 cycles were considered to be below the level of detection.

5′-Rapid amplification of cDNA ends (RACE)

To determine the transcriptional start sites of human aromatase transcripts from various tissues, 5′-RACE was performed using the SMART RACE cDNA amplification kit (CLONTECH, Mountain, CA) as described previously (12). The primary touchdown PCR reverse primers used were as follows: mouse touchdown reverse primer (5′-GACTCTCAT-GAATTCTCCATA CATCT-3′) and human touchdown reverse primer (5′-GTCCAATTCCCATGCAGTAGCCAGGA-3′). If the primary PCR reaction failed to give the distinct bands of interest, a secondary, or nested″ PCR was performed with the mouse nested reverse primer (5′-AATGAGGGGCCCAATTC-CCAGA-3′) and human nested reverse primer (5′-CCAA-GAGAAAAAGGCCAGTGAGGAGCA-3′). RACE products were cloned into the pCR-TOPO TA cloning vector and subsequently sequenced.

Exon-specific RT-PCR amplification

Total RNA was extracted from 24-wk-old left inguinal mammary gland (gland no. 4), and cDNA was synthesized using oligo(deoxythymidine) primers with a reverse transcriptase kit (Invitrogen, Camarillo, CA). To amplify the human transcript variants in the mammary gland (driven by promoters PII, I.3, and I.4), we used forward primers designed to hybridize to the different 5′-untranslated regions of each transcript and a reverse primer that hybridized to coding exon III (24). The PCR was run as follows: 4 min at 95 C, followed by 35 cycles of 30 sec at 94 C, 30 sec at 60 C, and 1 min at 72 C, and a final extension of 9 min at 72 C.

Whole mounts, tissue histology, and immunohistochemistry

The morphology of the mammary glands was examined using the whole-mount technique (25). Glands were spread on glass slides, fixed, and subjected to carmine (Sigma Chemicals) staining. To prepare mammary gland sections, inguinal glands were removed from mice, fixed in 4% phosphate-buffered paraformaldehyde overnight, and then transferred to 70% ethanol. Tissues were embedded in paraffin and sectioned at 5 μm. After deparaffinization, rehydration, and antigen retrieval by heating in antigen unmasking solution (Vector Laboratories, Burlingame, CA), primary antibodies [human aromatase (1:100, MCA 2077); AbD Serotec, Oxford, UK; or Ki67 antibody (1:200, ab66155); Abcam, Cambridge, MA] were applied to the sections. After incubation at 37 C for 1 h or 4 C overnight, the sections were washed with PBS and incubated with a biotinylated horse-antimouse secondary antibody (1:600, BA-2000;Vector Laboratories) at 37 C for 30 min followed by avidin-biotin-horseradish peroxidase complex (Vector, Laboratories). Sections were examined using a Zeiss Axio Scope microscope (Zeiss, Gottingen, Germany) (26).

Protein extraction and immunoblotting

Mammary gland total protein was extracted in a buffer containing 10 mmol/liter Tris (pH 7.4), 150 mmol/liter NaCl, 1 mmol/liter EDTA, 1 mmol/liter EGTA, 0.5% Nonidet P-40, protease inhibitors (2 mmol/liter phenylmethylsulfonyl fluoride, 10 mg/ml leupeptin, and 10 mg/ml aprotinin), and phosphatase inhibitors (100 mmol/liter sodium fluoride, 10 mmol/liter sodium pyrophosphate, and 2 mmol/liter sodium orthovanadate). Lysates were centrifuged at 50,000 × *g* for 60 min at 4 C. Protein concentrations were determined using the bicinchoninic acid protein assay (Pierce, Rockford, IL) according to the manufacturer's instructions. Samples containing 25 μg of protein were boiled for 4 min in a reducing Laemmli sample buffer containing 80 mmol/liter dithiothreitol and subjected to electrophoresis on 10% sodium dodecyl sulfate-polyacrylamide gels. Proteins were then transferred from gels to nitrocellulose membrane. The membranes were blocked with 5% insulin-free BSA in TBS-Tween 20, and proteins were detected using various antibodies [phospho-Stat5 (1:500, 71-6900) and Stat5a (1:1000, 13-3600) antibodies (Invitrogen); β-casein (H-7) antibody (1:500, sc-166520) (Santa Cruz Biotechnology, Santa Cruz, CA); and β-actin antibody (1:6000, A1978) (Sigma Chemicals)]. After extensive washings, the immune complexes were detected with horseradish peroxidase conjugated with specific secondary antiserum [(1:5000, antirabbit IgG (7074), antimouse IgG (7076); Cell Signaling Technology, Inc., Danvers, MA)] followed by an enhanced chemiluminescence reaction. The blots were analyzed by densitometry and quantified with MultiGauge software (Fuji PhotoFilm, Valhalla, NY).

Serum and tissue hormone levels

Blood samples were obtained from the retroorbital vein or tail vein. Serum estradiol (E_2) was measured by ELISA (ES 180S; Calbiotech Inc., Spring Valley, CA), serum testosterone, progesterone, and FSH levels were measured by RIA, and LH was measured by immunoradiometric assay by the University of Virginia Center for Research in Reproduction Ligand Assay and Analysis Core (Charlottesville, VA) (27–30). The mouse LH and FSH

assays are in the Methods section of the web site of this facility (http://www.medicine.virginia.edu/research/institutes-and-programs/crr/lab-facilities/assay-methods-page). Estrogens [estrone (E_1) and E_2] and estrogen metabolites [2-methoxyestrone ($2ME_1$), 2-methoxyestradiol ($2ME_2$) and estriol (E_3)] in serum and the mammary gland were determined by liquid chromatography-tandem mass spectrometry (LC-MS^2) at the National Cancer Institute/National Institutes of Health, as described previously (31). Serum prolactin levels were measured by bioassay (32). The determination of the stage of the estrous cycle was made by vaginal smears. To measure serum E_2 levels by ELISA at various stages of the estrous cycle (Calbiotech), serum from 6.5-wk-old mice was collected for 8–9 consecutive days from the tail vein.

Superovulation

Pregnant mares' serum gonadotropin (PMSG) and human chorionic gonadotropin (HCG) was obtained from Sigma Chemicals. Ten 8-wk-old mice for each genotype [wild type (WT), F1772, F1771] were injected ip with 5 IU PMSG. Forty-eight hours after the PMSG injection, five of each genotype were killed and ovaries were collected. The other five were injected ip with 5 IU HCG. Sixteen hours after the HCG injection, the second five mice were killed and ovaries were collected for the further investigation. Five 8-wk-old mice for each genotype were injected with vehicle alone as controls.

Vaginal opening and estrous cyclicity

Beginning 10 d after birth, females were examined daily for the onset of vaginal opening. To examine various stage of the estrous cycle, vaginal lavages with 0.9% NaCl from female mice (6.5–8 wk old) were obtained and viewed under a microscope daily between 0900 and 1000 h for at least two cycles (8–9 consecutive days). A normal estrous cycle was defined as 2 d of leukocytic cytology followed by 1 d of nucleated and 1–2 d of cornified cytology.

Statistical analysis

Results are expressed as mean ± SE. Statistically significant differences at $P < 0.05$ were determined using a one-factor ANOVA followed by a *t* test.

Results

Generation of the transgenic Arom^hum mouse

To develop an animal model in which the human aromatase gene is regulated via its tissue-specific alternative promoters in various tissues, we first screened and obtained a human BAC clone containing the human aromatase coding sequence flanked by its full-length, 93-kb 5'-regulatory region and the 3'-polyadenylation site. We injected a single copy of the BAC clone into pronuclear mouse embryos to generate the Arom^hum transgenic mouse line. PCR primers designed to amplify the human aromatase coding region and the major promoter sequences were used to identify six initial founders containing the transgene. A schematic of the human BAC clone

construct used to generate the Arom^hum line and a representative PCR of genomic DNA from two of the six founders (F1772 and F1771) are shown in Fig. 1A. Both F1772 and F1771 harbored the full (30 kb) coding region and its 3' end. F1772 had a 4.3-kb 5'-flanking region containing only the proximal promoters I.6 and I.3/II, whereas F1771 included a greater than 78-kb 5'-flanking region encompassing the more distal promoters I.4, I.7, and I.f as well as promoters I.6 and I.3/PII (Fig. 1A). As in humans, the encoded aromatase protein was identical in both founders, regardless of the promoters present in the transgene.

To determine the aromatase mRNA expression profile in female Arom^hum mouse tissues, 24-wk-old mice were euthanized and multiple tissues were collected and analyzed using real-time RT-PCR (Table 1). Consistent with patterns of extragonadal aromatase expression in women, human aromatase mRNA was detected in the ovary, hypothalamus, pituitary, uterus, mammary gland, aorta, lung, stomach, adrenal gland, bladder, gonadal fat, sc fat, and abdominal muscle in both F1771 and F1772 Arom^hum mouse lines and in the quadriceps muscle, brown adipose tissue, heart, liver, spleen, intestine, kidney, and bone in the F1771 line (Table 1). We used 5'-RACE to detect promoter-specific mRNA species. The term *present* denotes only the amplification of the coding region of human aromatase mRNA species by real-time PCR; we were, however, unable to detect promoter-specific 5'-untranslated regions in these tissues using 5'-RACE. If 5'-RACE produced a promoter-specific mRNA, this promoter was indicated in Table 1. Mouse aromatase mRNA in the ovary and brain was similar between WT and Arom^hum mice (Supplemental Fig. 1). In the ovary aromatase is mainly expressed in granulosa cells. Arom^hum mice showed strong expression of human aromatase mRNA in the ovary. We used PMSG in conjunction with HCG to superovulate female mice. Both mouse and human aromatase mRNA levels were significantly increased in WT, F1772, and F1771 mice after administration of PMSG for 48 h and significantly decreased in all mice after HCG injection for 16 h compared with PSMG treatment (Fig. 1, B and C). These data demonstrated that both the aromatase transgene and endogenous aromatase have a similar expression pattern. The endogenous mouse aromatase was lower in PMSG-treated F1772 mice as compared with PMSG-treated WT and F1771 mice but was higher compared with vehicle-treated F1772 mice (Fig. 1, B and C). Thus, the human transgene did not change the general pattern of endogenous aromatase expression. To determine the fertility/reproductive function of Arom^hum mice, transgenic and WT females were mated with WT males. The average litter size between WT and Arom^hum mice was similar (Fig. 1D). Ovarian appearance, including the number of
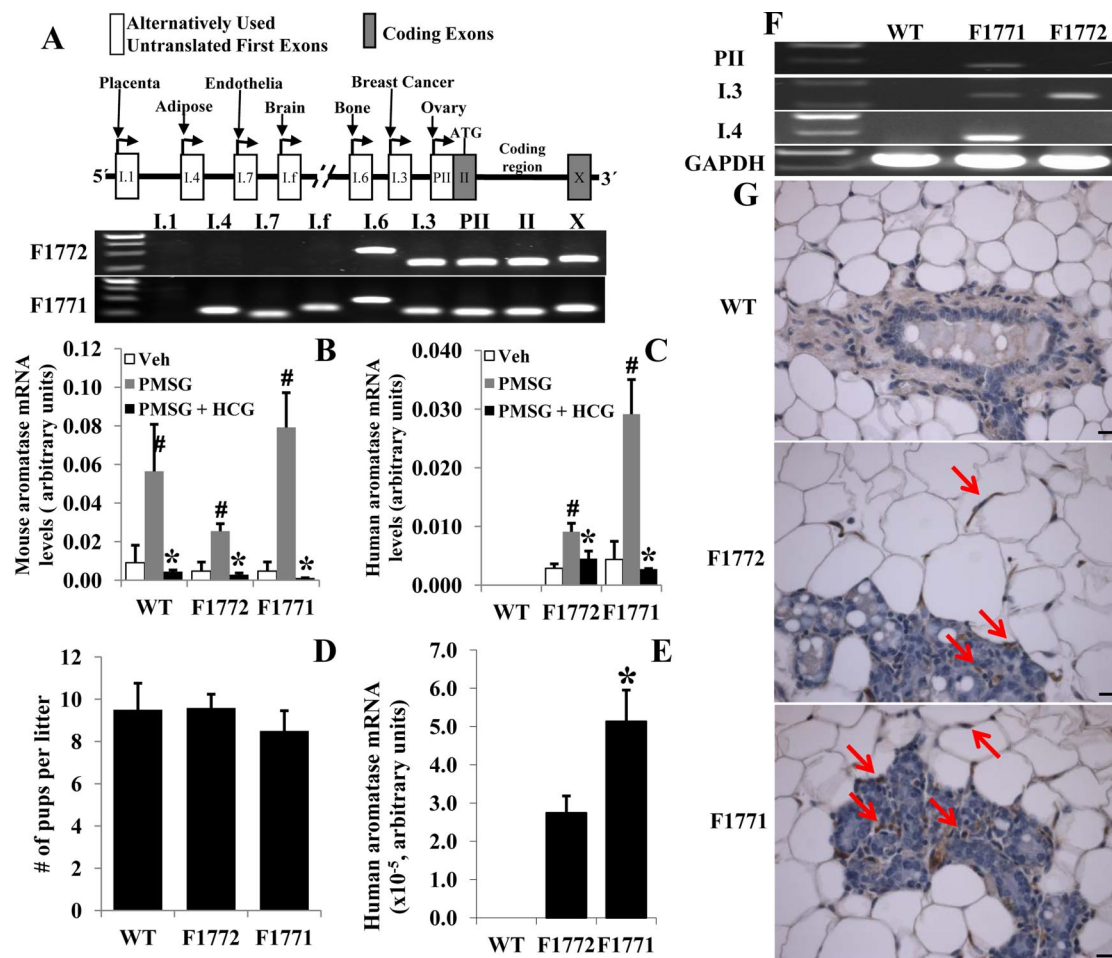
FIG. 1. Generation and characterization of the Arom[hum] transgenic mouse line. A, Schematic of the human BAC clone construct used to generate Arom[hum] transgenic mice. RT-PCR showed transmission of the transgene to the germline. F1772 contained exons PII, I.3, and I.6. F1771 contained all first exons of the aromatase gene except I.1. Mouse (B) and human (C) aromatase mRNA levels in ovaries of superovulated mice are shown. Females were given one of the following: 1) PMSG for 48 h, 2) PMSG for 48 h followed by HCG for 16 h, or 3) vehicle (Veh) alone. Ovaries were collected after treatment for the further analysis as described in *Materials and Methods* (n = 5 mice per group). #, $P < 0.05$ *vs.* vehicle; *, $P < 0.05$ *vs.* PMSG. D, Average litter size of Arom[hum] or WT females mated to WT males (n = 8 mice per group). E, Human aromatase mRNA was expressed in the mammary glands of Arom[hum] mice. *, $P < 0.05$. F, Exon-specific RT-PCR confirmed the different promoter driven human aromatase expression in the mammary gland of Arom[hum] mice. GAPDH mRNA levels served as the control. Data are representative of three independent experiments. G, Immunohistochemical localization of human aromatase in the mammary glands of Arom[hum] mice (n = 4–5 mice per group). *Arrows* indicate aromatase positive staining. *Bar*, 50 μm.

corpus lutea (ovulation), was similar between WT and Arom[hum] mice (data not shown).

Expression of human aromatase in mammary adipose fibroblasts and myoepithelia of Arom[hum] mice via its cognate promoters PII, I.3, and I.4

We next analyzed each of the transgenic lines for the expression and promoter usage of aromatase in mammary gland. Total RNA was isolated from biopsies of inguinal mammary glands (no. 4) from 24-wk-old Arom[hum] and WT littermates. In Arom[hum] mice, we found human aromatase expression in mammary gland and that the level of human aromatase mRNA was significantly higher in F1771 mice than that in F1772 mice (Fig. 1E). Human aromatase mRNA was not detected in the WT mammary

glands. We then used exon-specific RT-PCR to determine promoter usage in the mammary gland of Arom[hum] mice and found that human aromatase expression was driven by PII, I.3, and I.4 in F1771 mice and by I.3 in F1772 mice (Fig. 1F). We used immunohistochemistry to localize human aromatase within the mammary gland of Arom[hum] mice; as expected, human aromatase immunostaining was absent in WT mice. In 24-wk-old Arom[hum] mice, staining was observed in adipose fibroblast cells and myoepithelial cells but absent in epithelial cells (Fig. 1G).

Increased local estrogen concentration in the breast tissue of Arom[hum] mice

To determine whether elevated human aromatase expression in the Arom[hum] mouse mammary tissue is ac-

TABLE 1.   mRNA expression profile of human aromatase in various tissues of 24-wk-old female Arom^hum mice

Tissues (n = 3)	WT		F1772		F1771	
	H Arom	M Arom	H Arom	M Arom	H Arom	M Arom
Ovary	—	Pgon	PII	Pgon	PII	Pgon
Hypothalamus	—	Pbr	Present	Pbr	I.f	Pbr
Pituitary	—	—	Present	—	Present-	—
Nonpregnant uterus	—	—	Present	—	Present-	—
Mammary gland	—	—	PII/I.3	—	PII/I.3/I.4	—
Aorta	—	—	Present	—	I.4	—
Lung	—	—	Present	—	I.4	—
Stomach	—	—	Present	—	Present-	—
Adrenal gland	—	—	Present	—	Present-	—
Bladder	—	—	Present	—	I.4	—
Gonadal fat	—	—	Present	—	Present-	—
Subcutaneous fat	—	—	Present	—	Present-	—
Abdominal muscle	—	—	Present	—	I.4	—
Quadriceps muscle	—	—	—	—	I.4	—
Brown adipose	—	—	—	—	Present-	—
Heart	—	—	—	—	Present-	—
Liver	—	—	—	—	Present-	—
Spleen	—	—	—	—	Present-	—
Intestine	—	—	—	—	I.7/I.f	—
Kidney	—	—	—	—	Present-	—
Bone	—	—	—	—	I.4	—

Quantitative real-time RT-PCR was used to determine the presence or absence (−) of mouse and human aromatase mRNA in various tissues of WT mice and lines F1772 and F1771. 5′-RACE identified mRNA transcribed from each promoter (PII, I.f, I.4, I.3) in the human aromatase transgene or native mouse promoters. Pgon, Mouse gonadal aromatase promoter; Pbr, mouse brain promoter; H Arom, human aromatase; M Arom, mouse aromatase.

companied by increased tissue estrogen levels and change in circulating hormone levels, we compared mammary tissue E_2 levels and peripheral serum levels of estrogens, progesterone, testosterone, prolactin, and the gonadotropins LH and FSH using ELISA and RIA technologies (Fig. 2). Serum E_2 levels were similar between WT, F1772, and F1771 females (Fig. 2A), as were those in the mammary tissue (data not shown). However, serum LH concentra-

tions were lower in F1771 by 57 and 37%, respectively, compared with WT and F1772 females (Fig. 2B). The decreased LH in the F1771 line also accounted for the significantly lower serum testosterone levels (Fig. 2D) and a nonsignificant trend of lower progesterone levels in F1771 females (Fig. 2E) because LH regulates ovarian progesterone secretion. Serum concentrations of FSH and prolactin remained unchanged between WT, F1772, and F1771 littermates (Fig. 2, C and F).

Because serum concentrations measured by ELISA of the biologically active estrogen, E_2, were not different between WT, F1772, and F1771 mice, we applied a much more sensitive technology, LS-MS^2, to measure the total serum concentrations of the estrogens (E_1 and E_2) and its metabolites (E_3, $2ME_1$, and $2ME_2$). Serum E_1 levels were slightly but significantly increased in F1772 and F1771 mice compared with WT mice (Fig. 3A). Serum E_2 and E_3 levels were also modestly but significantly higher in F1772 mice compared with WT mice. However, the total levels of estrogens were similar between WT, F1772, and F1771 females,
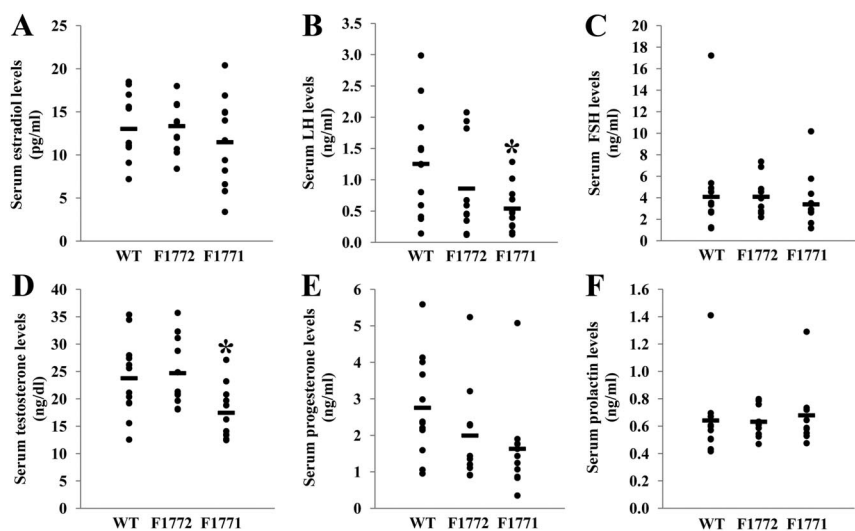
FIG. 2. Serum testosterone and LH levels are lower in Arom^hum mice compared with WT littermates. Mouse sera were collected from 24-wk-old mice. Serum E_2 (A), LH (B), FSH (C), testosterone (D), progesterone (E), and prolactin (F) were measured by ELISA, RIA, or bioassay (n = 11–12 mice per group). *, $P < 0.05$ *vs.* WT mice.
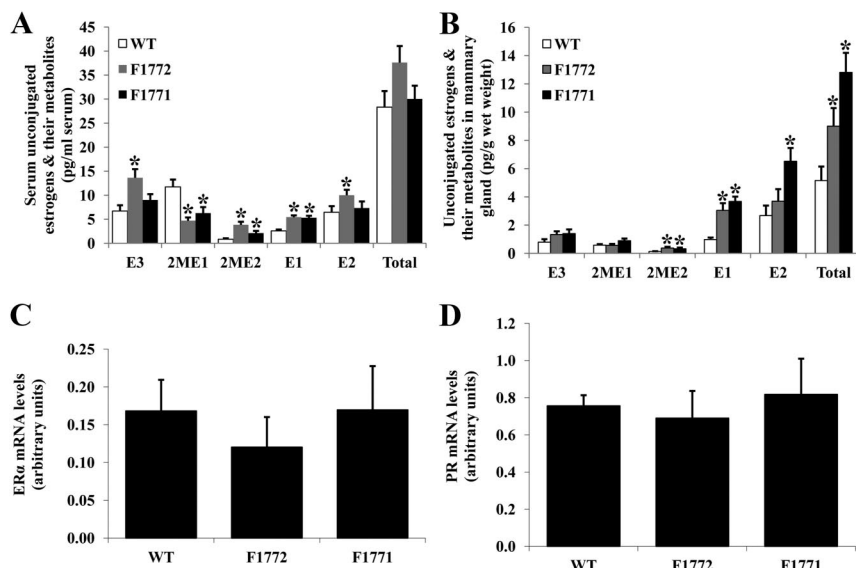
FIG. 3. Mammary unconjugated estrogens are higher in Arom[hum] mice compared with WT littermates. Serum (A) and mammary gland (B) unconjugated estrogens and estrogen metabolites were measured by LC-MS^2 assay. E_1, E_2, E_3, $2ME_1$, and $2ME_2$ are shown. mRNA levels of ERα (C) and PR (D) were measured by real-time RT-PCR (n = 15 mice per group). *, $P < 0.05$ vs. WT mice.

which concurred with E_2 levels measured by ELISA (Fig. 2A). Serum $2ME_1$ levels were significantly decreased and $2ME_2$ levels were significantly increased in F1772 and F1771 mice compared with WT mice.

To determine the functionality of human aromatase transgene and production of estrogens in the mammary gland, we also measured the local levels of mammary estrogens and their metabolites using LS-MS^2 (Fig. 3B). Total mammary estrogen levels were significantly higher in F1772 by 1.8-fold and in F1771 by 2.5-fold, compared with WT mice (Fig. 3B). Compared with WT mice, E_1 levels were 3.1-fold higher in F1772 and 3.8-fold higher in F1771 mice; E_2 levels were 1.4-fold higher in F1772 and 2.4-fold higher in F1771 mice; and $2ME_2$ levels were significantly higher in F1772 and F1771 mice ($P < 0.05$). No differences in mammary E_3 or $2ME_1$ levels were observed between WT, F1772, and F1771 mice (Fig. 3B). ERα and progesterone receptor (PR) mRNA levels did not differ between WT, F1772, and F1771 mice (Fig. 3, C and D).

Increased ductal elongation and outgrowth during puberty in Arom[hum] mice

E_2 has been shown to act directly on the mammary gland to stimulate ductal elongation during puberty (33). To determine whether expression of human aromatase in the mammary gland affects ductal morphogenesis, we observed mammary morphological changes in mice at 5, 7, or 12 wk of age. At 5 wk of age (prepubertal), the size and morphology of the mammary glands from WT and Arom[hum] mice were similar (Fig. 4C). At 7 wk of age (equivalent

to puberty), mammary tissues from both WT and Arom[hum] showed similar morphological changes, with prominent duct elongation and a few alveoli growing from terminal branches at the end buds; however, ductal outgrowth was accelerated in F1771 mice compared with WT mice. We measured the ductal length from the mammary lymph node to the tip of the terminal end buds in 7-wk-old mice and found that mammary ducts of F1771 mice were significantly longer than those of WT mice (Fig. 4, A and B). Mammary gland morphology and ductal elongation were similar in WT and Arom[hum] mouse lines at 12 wk of age (postpubertal, Fig. 4C). The vaginal opening, an external marker for the onset of puberty, was first observed at similar ages in WT, F1772, and F1771 mice (29.8 ± 0.4, 30 ± 0.8, and 29.2 ± 0.4 d, respectively; n = 6, Fig. 4D). These data suggest that the observed increase in ductal length in the F1771 lines cannot be explained by early puberty. Serum E_2 levels at the proestrous stage of WT and Arom[hum] mice were significantly higher than the serum E_2 levels at diestrous or estrous stages. However, the serum E_2 levels were not different between WT, F1772, and F1771 mice within the same estrous stage (Fig. 4E). This result suggested that the accelerated ductal growth at puberty is not secondary to increased serum estrogen levels but more likely due to excess local estrogen production in the mammary gland.

Mammary aromatase expression and estrogen production are associated with mammary hyperplasia in Arom[hum] mice

We showed that the Arom[hum] mice express human aromatase in several peripheral tissues, including breast fat, under the control of alternative promoters and produce estrogen in the mammary glands, mimicking human patterns of extraovarian estrogen production. To determine the effects of local estrogen on breast tissue in the Arom[hum] mouse, we analyzed mouse mammary morphology and histology at 24 and 64 wk of age. Figure 5A shows whole-mount staining of mammary glands at 24 wk of age. Virgin WT females exhibited normal mammary ductal morphogenesis as reflected by the presence of an ordered ductal network with normal side branching. In contrast, virgin Arom[hum] mice displayed disseminated mammary gland hyperplasia indicated by excessive ductal side branching
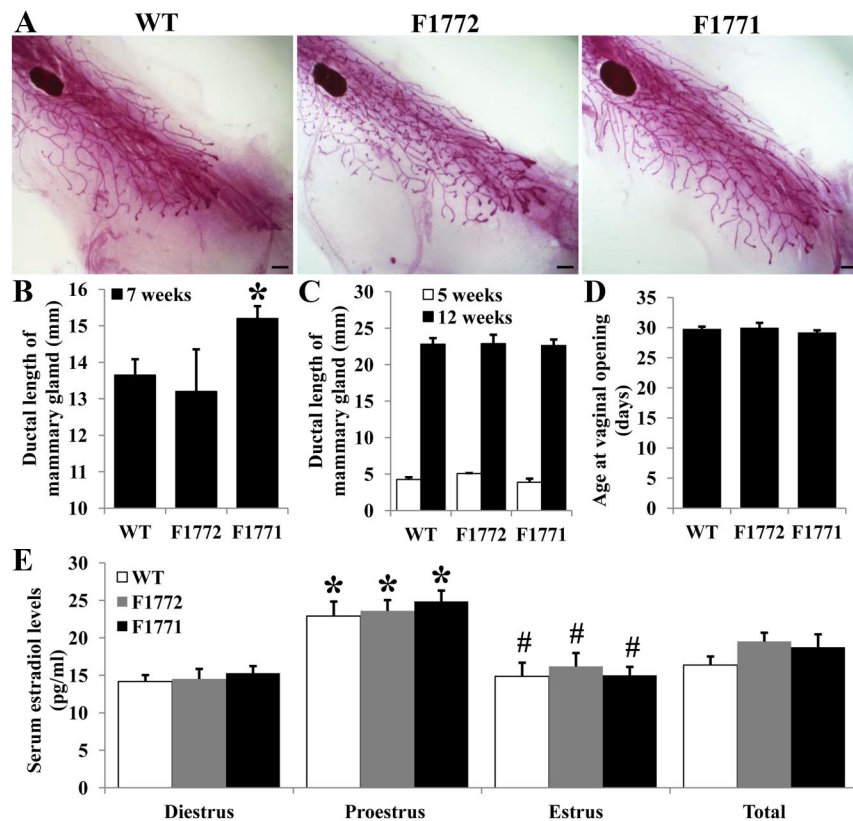
FIG. 4. Increased mammary ductal elongation during puberty in F1771 Arom[hum] mice compared with WT mice. A, Whole-mount staining was performed on mammary glands from WT, F1772, and F1771 mice at 7 wk of age. Glands were spread on glass slides, fixed, and subjected to carmine staining. *Bar*, 1000 μm. B, The length of mammary ducts from 7-wk-old (B) and 5- and 12-wk-old females (C) were measured from the lymph node to the tip of the terminal end buds. D, The time of vaginal opening in Arom[hum] mice was not different from littermate controls (n = 6 mice per group). E, Serum E_2 levels were measured based on cycle stage. The 6.5-wk-old mice were bled for 8–9 consecutive days. Cycle stage was determined by vaginal cytology (n = 10–11 mice per group). *, $P < 0.01$ *vs.* diestrous stage; #, $P < 0.05$ *vs.* proestrous stage.
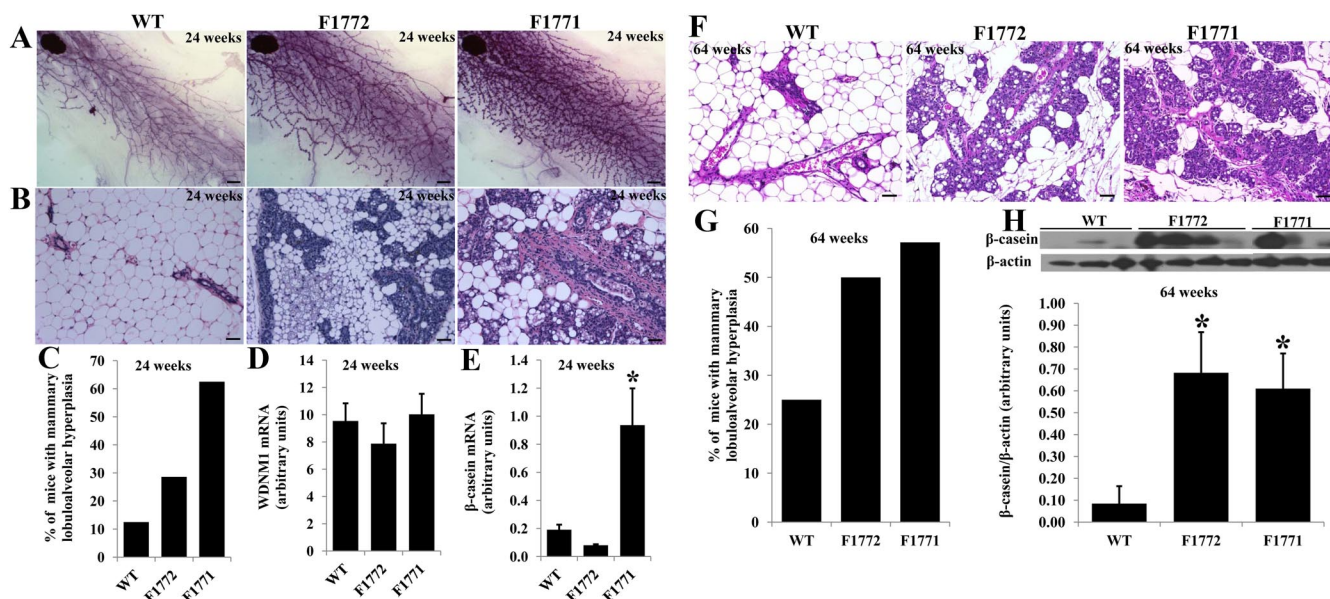
tween WT, F1772, and F1771 mice (Fig. 5, D and E). To minimize differences on mammary gland histology and milk protein levels resulting from the estrous cycle, postmenopausal female (64 wk old) mammary glands were analyzed. Lobuloalveolar hyperplasia in Arom[hum] mice had a similar appearance at both 24 and 64 wk old (Fig. 5, B and F). However, the percent of mice exhibiting hyperplasia was higher in WT and F1772 mice at 64 wk of age compared with that at 24 wk of age and similar in 1771 mice between 24 and 64 wk old (Fig. 5, C and G). Milk protein β-casein was significantly increased in 64-wk-old Arom[hum] as compared with the WT littermates (Fig. 5H).

Mammary hyperplasia is induced by epithelial hyperproliferation in Arom[hum] mice

We observed a significantly higher epithelial cell content in the mammary glands of Arom[hum] mice compared with WT mice, which may be due to an increase in estrogen-stimulated epithelial proliferation. We performed Ki67 immunohistochemical analysis to compare the level of epithelial cell proliferation in the mammary glands of WT and Arom[hum] mouse lines. The numbers of Ki67-positive nuclei in the mammary epithelium of Arom[hum] mouse lines were significantly higher than those in WT mice at 24 wk of age (Fig. 6, A and C). Specifically, the percentage of Ki67-positive nuclei was 4.8-fold and 2.8-fold higher in the mammary epithelium of F1771 and F1772 mice, respectively, compared with WT mice ($P < 0.05$ for both). We performed Ki67 immunohistochemistry in postmenopausal female mice (64 wk old) to preclude the variation resulting from the estrous cycle. The percentage of Ki67-positive nuclei was similar between 24- and 64-wk-old WT, F1772, and F1771 mice (Fig. 6, B and D).

Mammary aromatase expression is associated with phosphorylation of Stat5 in Arom[hum] mice

To better understand the activated signaling pathways associated with increased local estrogens production in breast tissue displaying hyperplasia and lipid droplets, we used immunoblotting to determine protein phosphorylation in mammary glands of 24-wk-old females. Previous

and by the development of aberrant lobular structures. However, mammary gland hyperplasia was reduced evidenced by decreased ductal side branching in F1772 mice as compared with F1771 mice. Mammary glands in Arom[hum] mice (F1772 and F1771 lines) showed a marked increase in lobuloalveolar hyperplasia and exhibited extensive lipid droplets at 24 wk compared with WT mice (Fig. 5B). Keratinizing hyperplasia was also seen in mammary glands of F1771 females (data not shown). The percent of mice in each group showing hyperplasia was 5-fold higher in F1771 mice and 3-fold higher in F1772 mice compared with WT mice (Fig. 5C). We also investigated whether the lobuloalveoli in the Arom[hum] mice were functional by measuring the expression levels of various milk-specific mRNA transcripts and protein during pregnancy (34). β-casein mRNA levels were significantly increased in F1771 mice compared with WT and F1772 mice; however, WDNM1 (also called extracellular proteinase inhibitor or Expi) mRNA levels were similar be-

FIG. 5. Mammary lobuloalveolar hyperplasia in the Arom^hum mouse. A, Whole-mount staining was performed on mammary glands from WT, F1772, and F1771 mice at 24 wk of age (n = 5 mice per group). *Bar*, 1000 μm. B, Hematoxylin and eosin (H&E) staining was performed on 24-wk-old mammary gland tissue from WT, F1772, and F1771 mice (n = 4 or 5 mice per group). *Bar*, 50 μm. C, Percentage of mice showing mammary hyperplasia was determined based on H&E staining of mammary glands from 24-wk-old mice (n = 11 mice per group). mRNA expression of milk proteins WDNM1 (D) and β-casein (E) in mammary glands of WT and Arom^hum mice was measured by real-time RT-PCR and normalized to GAPDH mRNA levels (n = 4 mice per group). *, $P < 0.05$ *vs.* WT mice. F, H&E staining was performed on 64-wk-old mammary gland tissue from WT, F1772, and F1771 mice (n = 4 or 5 mice per group). *Bar*, 50 μm. G, Percentage of mice showing mammary hyperplasia from 64-wk-old mice (n = 5 mice per group). H, Milk protein β-casein was measured by Western blotting in WT and Arom^hum mice at 64 wk of age (n = 3–4 mice per group).

studies showed that estrogens, via binding to cytoplasmic or membrane receptors, rapidly activated intracellular signaling cascades such as Stat, ERK, or PI3K/Akt (35, 36). As shown in Fig. 7, A and B, Western blot analysis showed a significant increase in Stat5a phosphorylation in breast tissue of F1771 mice compared with WT mice at the age of 24 wk. Stat5 phosphorylation in postmenopausal females (64 wk) was measured to preclude possible cycle stage-dependent variations. Similar differences were observed between 24-wk-old and 64-wk-old mice (Fig. 7, C and D). Stat5a phosphorylation in F1772 mice was also increased at 24 and 64 wk of age, but this difference was not statistically significant. Phosphorylation of ERK or Akt was not detectable in WT, F1772, or F1771 mice (data not shown).

Discussion

We and others have shown that two distinct promoters control aromatase expression in the ovary and brain of female mice (12–14). However, additional alternative promoters regulate aromatase expression in many extragonadal tissues (*e.g.* fat in breast, bone, and lung) in women (11, 37). To mimic the human aromatase expression patterns and physiology related to local estrogen pro-duction in various tissues, we generated Arom^hum mouse lines containing a single copy of the human aromatase gene driven by its native tissue-specific promoters. The aromatase expression pattern in Arom^hum mammary stroma and myoepithelia mimicked human aromatase expression in basal and stromal cells in human breast tissues (38). The Arom^hum mice produced excessive local estrogen in breast tissue and displayed mammary lobuloalveolar hyperplasia at 24 and 64 wk. This new mouse model is the first of its kind. We predict that it will be a valuable tool for developing tissue-specific aromatase inhibition strategies.

The mammary gland undergoes most of its branching during adolescence rather than during fetal development. Hormone-dependent branching requires estrogen and ERα expression in the breast (33). In this study, human aromatase expression in mouse mammary stroma and myoepithelia was associated with increased local estrogen production and increased ductal elongation and outgrowth in the mammary gland during puberty compared with WT littermates. However, WT and Arom^hum mice had similar levels of serum estrogens, suggesting an important role of local excessive mammary tissue estrogens in stimulating linear ductal growth at puberty. These results are inconsistent with previous reports that described
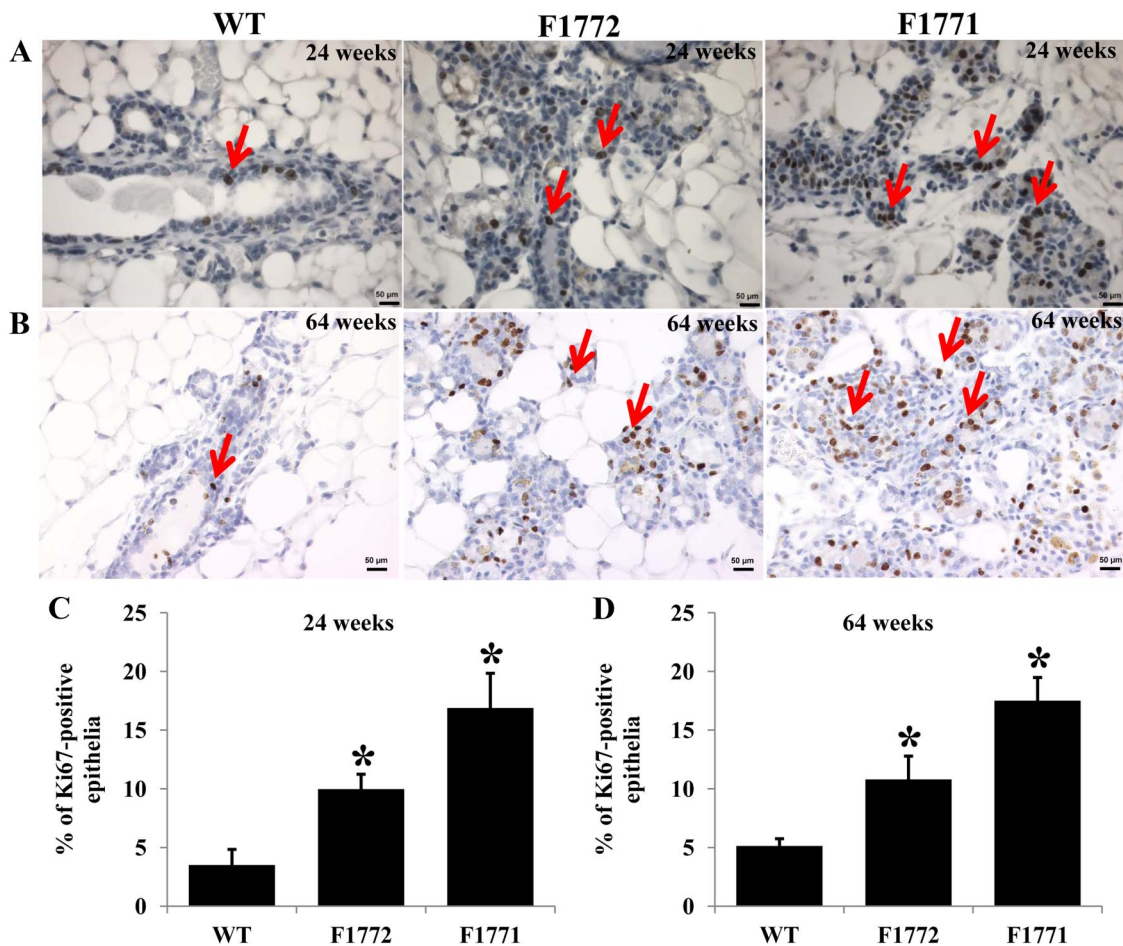
FIG. 6. Cell proliferation evaluated by Ki67 staining is higher in mammary epithelia of Arom[hum] mice compared with WT littermates. Ki67-positive nuclei were detected at 24 wk (A) and 64 wk (B) of WT, F1772, and F1771 mice by immunostaining using an antibody against Ki67 (*arrows*). *Bar*, 50 μm. A total of 2000 nuclei were counted in sections obtained from mice at 24 wk (C) and 64 wk of age (D) to calculate the percent of Ki67-positive nuclei in WT and Arom[hum] mice (n = 3–4 in each group). *, $P < 0.05$ *vs.* WT.

a role of systemic estrogen rather than local estrogen in controlling mammary side branching (39).

Aromatase converts the androgens testosterone and androstenedione into E_2 and E_1, respectively. As expected, humanized aromatase expression decreased systemic testosterone levels in the Arom[hum] mice, which was most likely caused by suppression of LH by the additional local production of estrogen driven by human aromatase expressed in the brain. Peripheral human aromatase expression probably does not account for the decreased testosterone in F1771 females because peripheral conversion of testosterone to E_2 is estimated to be approximately 1% (11). A previous study showed that estrogens induced PR expression and increased pituitary prolactin concentration (39, 40). However, in the present study, additional estrogen production from the human aromatase gene did not change circulating levels of prolactin, progesterone or FSH nor did this effect on mRNA levels of PR or ERα in the mammary gland. These results suggest that elevated

tissue estrogen production exerts selective effects on certain endocrine systems.

The Arom[hum] mice, containing a single copy of the entire human aromatase gene, mimicked human aromatase expression pattern in mice and thus human physiology with respect to estrogen production (41). This Arom[hum] mouse model is unique and offers new opportunities for studying estrogen-related physiology for the following reasons. Because the Arom[hum] mice were generated via autosomal insertion of a single copy of the entire human aromatase gene, it produces physiological amounts of estrogen in relevant mouse tissues. Second, the tissue distribution pattern of human aromatase expression in Arom[hum] females is nearly identical with that observed in women. Third, physiologically relevant native promoters control the human aromatase gene in a tissue-selective fashion. Fourth, the physiological genetic mechanisms such as binding of transcriptional activator or silencer complexes to the native chromatin leading to alternative
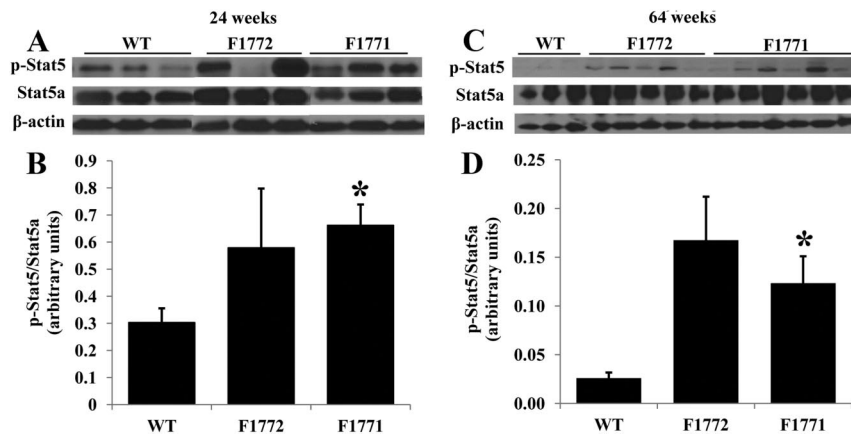
FIG. 7. Stat5 phosphorylation is increased in mammary gland of Arom^{hum} mice. Representative Western blot analysis in 24-wk-old (A) and 64-wk-old (C) and quantification of phosphorylated Stat5 in 24-wk-old (B) and 64-wk-old (D) mammary gland of WT and Arom^{hum} mice are shown. Mammary gland protein extracts from WT and Arom^{hum} mice (25 μg proteins per sample) were subjected to immunoblot analysis using an antibody against phosphorylated Stat5, Stat5a, and β-actin, as described in *Materials and Methods* (n = 3–6 mice in each group). *, $P < 0.05$ *vs.* WT.

activation of promoters, alternative splicing of an untranslated first exon to a common splice junction, and the rest of the splicing events leading mRNA transcription and its polyadenylation, all operate in a seemingly identical fashion to that observed in the human body. Finally, the cellular distribution of the aromatase expression in the mammary tissue of mice matched our previously published observation in women (42).

The insertion of a single copy of the human aromatase gene into female mice gave rise to a remarkably increased frequency of lobuloalveolar hyperplasia in the mammary tissue, which was accompanied by increased mammary epithelial proliferation at 24 wk of age. Although these findings may be associated with an increased risk of malignancy in the long term, the incidence of mammary cancer in these mice is currently unknown. It may be necessary to facilitate carcinogenesis chemically or by crossing these mice with a mildly tumorigenic genetic strain to assess the role of the human aromatase gene in mammary carcinogenesis. This will be an active area of research in our laboratory.

Prolactin plays a primary role in the physiological process of mammary gland secretion through the activation of various signaling cascades including Janus kinase-2/Stat5, ERK, and PI3K/Akt (43). Stat5 was first found to be involved in the prolactin-induced β-casein gene expression in mammary glands (44). Here we observed lipid droplet accumulation in the mammary glands of Arom^{hum} mice. However serum prolactin levels were similar in WT and Arom^{hum} mice. Previous studies have shown that estrogens, via binding to cytoplasmic or membrane receptors, rapidly activated intracellular signaling cascades such as Stat, ERK, or PI3K/Akt (35, 36). Stat5a phosphorylation

was significantly increased in breast tissue of F1771 mice compared with WT mice. However, not every mouse showed the increased of Stat5 phosphorylation. This may be due to expected variations in gene expression and signal transduction in transgenic mice, which are frequently encountered. These data suggested that local increased E$_2$ could activate Stat5 and that this could be a mechanism for mammary hyperplasia and lipid droplet accumulation.

The side effects observed during treatment with the aromatase inhibitors are the result of global inhibition of the aromatase activity in all tissues (18, 45, 46). Thus, the ideal therapeutic approach to treatment of estrogen-responsive breast cancers would be the tissue-specific blockage of estrogen production in the breast only. The development of tissue-selective aromatase inhibitors is plausible because of the tissue-specific regulation of aromatase expression (47, 48). Inhibition of promoter II/I.3-mediated transcription might provide a breast-specific therapy (20, 49); therefore, factors regulating transcription from these promoters are currently being studied. Because aromatase expression in the Arom^{hum} model closely resembles that in humans, the model may be useful for identifying signaling pathway inhibitors that can block aromatase expression arising from promoters II and I.3 but permit the activation of promoters I.f, I.4, and I.6. This would lead to the inhibition of all estrogen synthesis in the ovary and the majority of estrogen synthesis in the mammary gland but permit local estrogen production in the brain, bone, and at low levels in fat. This approach would be sufficient to inhibit mammary hyperplasia and carcinogenesis while maintaining the beneficial effects of estrogen in other tissues. Such an approach may lead to viable treatment options with fewer side effects compared with the currently available aromatase inhibitor that causes whole-body estrogen deprivation. Our *in vivo* Arom^{hum} model would be ideal for screening candidate selective aromatase inhibitors.

Acknowledgments

References

1. Lubahn DB, Moyer JS, Golding TS, Couse JF, Korach KS, Smithies O 1993 Alteration of reproductive function but not prenatal sexual development after insertional disruption of the mouse estrogen receptor gene. Proc Natl Acad Sci USA 90:11162–11166

2. Krege JH, Hodgin JB, Couse JF, Enmark E, Warner M, Mahler JF, Sar M, Korach KS, Gustafsson JA, Smithies O 1998 Generation and reproductive phenotypes of mice lacking estrogen receptor beta. Proc Natl Acad Sci USA 95:15677–15682

3. Fisher CR, Graves KH, Parlow AF, Simpson ER 1998 Characterization of mice deficient in aromatase (ArKO) because of targeted disruption of the cyp19 gene. Proc Natl Acad Sci USA 95:6965–6970

4. Simpson ER 2000 Biology of aromatase in the mammary gland. J Mammary Gland Biol Neoplasia 5:251–258

5. Simpson ER, Mahendroo MS, Means GD, Kilgore MW, Hinshelwood MM, Graham-Lorence S, Amarneh B, Ito Y, Fisher CR, Michael MD, *et al.* 1994 Aromatase cytochrome P450, the enzyme responsible for estrogen biosynthesis. Endocr Rev 15:342–355

6. Czajka-Oraniec I, Simpson ER 2010 Aromatase research and its clinical significance. Endokrynol Pol 61:126–134

7. Kirma N, Gill K, Mandava U, Tekmal RR 2001 Overexpression of aromatase leads to hyperplasia and changes in the expression of genes involved in apoptosis, cell cycle, growth, and tumor suppressor functions in the mammary glands of transgenic mice. Cancer Res 61:1910–1918

8. Fox EM, Bernaciak TM, Wen J, Weaver AM, Shupnik MA, Silva CM 2008 Signal transducer and activator of transcription 5b, c-Src, and epidermal growth factor receptor signaling play integral roles in estrogen-stimulated proliferation of estrogen receptor-positive breast cancer cells. Mol Endocrinol 22:1781–1796

9. Santos SJ, Haslam SZ, Conrad SE 2008 Estrogen and progesterone are critical regulators of Stat5a expression in the mouse mammary gland. Endocrinology 149:329–338

10. Boon WC, Chow JD, Simpson ER 2010 The multiple roles of estrogens and the enzyme aromatase. Prog Brain Res 181:209–232

11. Bulun SE, Lin Z, Imir G, Amin S, Demura M, Yilmaz B, Martin R, Utsunomiya H, Thung S, Gurates B, Tamura M, Langoi D, Deb S 2005 Regulation of aromatase expression in estrogen-responsive breast and uterine disease: from bench to treatment. Pharmacol Rev 57:359–383

12. Zhao H, Innes J, Brooks DC, Reierstad S, Yilmaz MB, Lin Z, Bulun SE 2009 A novel promoter controls Cyp19a1 gene expression in mouse adipose tissue. Reprod Biol Endocrinol 7:37

13. Golovine K, Schwerin M, Vanselow J 2003 Three different promoters control expression of the aromatase cytochrome p450 gene (cyp19) in mouse gonads and brain. Biol Reprod 68:978–984

14. Honda S, Harada N, Takagi Y 1996 The alternative exons 1 of the mouse aromatase cytochrome P-450 gene. Biochim Biophys Acta 1305:145–150

15. Li X 2010 Aromatase over expression transgenic murine models for aromatase inhibitor studies. Mol Hum Reprod 16:80–86

16. Tekmal RR, Ramachandra N, Gubba S, Durgam VR, Mantione J, Toda K, Shizuta Y, Dillehay DL 1996 Overexpression of int-5/aromatase in mammary glands of transgenic mice results in the induction of hyperplasia and nuclear abnormalities. Cancer Res 56:3180–3185

17. Li X, Wärri A, Mäkelä S, Ahonen T, Streng T, Santti R, Poutanen M 2002 Mammary gland development in transgenic male mice expressing human P450 aromatase. Endocrinology 143:4074–4083

18. Gaillard S, Stearns V 2011 Aromatase inhibitor-associated bone and musculoskeletal effects: new evidence defining etiology and strategies for management. Breast Cancer Res 13:205

19. Brown KA, Simpson ER 2010 Obesity and breast cancer: progress to understanding the relationship. Cancer Res 70:4–7

20. Chen D, Reierstad S, Lu M, Lin Z, Ishikawa H, Bulun SE 2009 Regulation of breast cancer-associated aromatase promoters. Cancer Lett 273:15–27

21. Miano JM, Kitchen CM, Chen J, Maltby KM, Kelly LA, Weiler H, Krahe R, Ashworth LK, Garcia E 2002 Expression of human smooth muscle calponin in transgenic mice revealed with a bacterial artificial chromosome. Am J Physiol Heart Circ Physiol 282:H1793–H1803

22. Sparwasser T, Gong S, Li JY, Eberl G 2004 General method for the modification of different BAC types and the rapid generation of BAC transgenic mice. Genesis 38:39–50

23. Schmittgen TD, Livak KJ 2008 Analyzing real-time PCR data by the comparative C(T) method. Nat Protoc 3:1101–1108

24. Lu M, Chen D, Lin Z, Reierstad S, Trauernicht AM, Boyer TG, Bulun SE 2006 BRCA1 negatively regulates the cancer-associated aromatase promoters I. 3 and II in breast adipose fibroblasts and malignant epithelial cells. J Clin Endocrinol Metab 91:4514–4519

25. Dupont J, Renou JP, Shani M, Hennighausen L, LeRoith D 2002 PTEN overexpression suppresses proliferation and differentiation and enhances apoptosis of the mouse mammary epithelium. J Clin Invest 110:815–825

26. Zhao H, Cui Y, Dupont J, Sun H, Hennighausen L, Yakar S 2005 Overexpression of the tumor suppressor gene phosphatase and tensin homologue partially inhibits wnt-1-induced mammary tumorigenesis. Cancer Res 65:6864–6873

27. Haisenleder DJ, Schoenfelder AH, Marcinko ES, Geddis LM, Marshall JC 2011 Estimation of estradiol in mouse serum samples: evaluation of commercial estradiol immunoassays. Endocrinology 152:4443–4447

28. Fallest PC, Trader GL, Darrow JM, Shupnik MA 1995 Regulation of rat luteinizing hormone β gene expression in transgenic mice by steroids and a gonadotropin-releasing hormone antagonist. Biol Reprod 53:103–109

29. Haavisto AM, Pettersson K, Bergendahl M, Perheentupa A, Roser JF, Huhtaniemi I 1993 A supersensitive immunofluorometric assay for rat luteinizing hormone. Endocrinology 132:1687–1691

30. Parkening TA, Collins TJ, Smith ER 1982 Plasma and pituitary concentrations of LH, FSH, and prolactin in aging C57BL/6 mice at various times of the estrous cycle. Neurobiol Aging 3:31–35

31. Ziegler RG, Faupel-Badger JM, Sue LY, Fuhrman BJ, Falk RT, Boyd-Morin J, Henderson MK, Hoover RN, Veenstra TD, Keefer LK, Xu X 2010 A new approach to measuring estrogen exposure and metabolism in epidemiologic studies. J Steroid Biochem Mol Biol 121:538–545

32. Kline JB, Clevenger CV 2001 Identification and characterization of the prolactin-binding protein in human serum and milk. J Biol Chem 276:24760–24766

33. Hennighausen L, Robinson GW 2005 Information networks in the mammary gland. Nat Rev Mol Cell Biol 6:715–725

34. Robinson GW, McKnight RA, Smith GH, Hennighausen L 1995 Mammary epithelial cells undergo secretory differentiation in cycling virgins but require pregnancy for the establishment of terminal differentiation. Development 121:2079–2090

35. **Arendt LM, Evans LC, Rugowski DE, Garcia-Barchino MJ, Rui H, Schuler LA** 2009 Ovarian hormones are not required for PRL-induced mammary tumorigenesis, but estrogen enhances neoplastic processes. J Endocrinol 203:99–110

36. **Santos SJ, Haslam SZ, Conrad SE** 2010 Signal transducer and activator of transcription 5a mediates mammary ductal branching and proliferation in the nulliparous mouse. Endocrinology 151:2876–2885

37. **Demura M, Demura Y, Ameshima S, Ishizaki T, Sasaki M, Miyamori I, Yamagishi M, Takeda Y, Bulun SE** 2011 Changes in aromatase (CYP19) gene promoter usage in non-small cell lung cancer. Lung Cancer 73:289–293

38. **Li Z, Luu-The V, Poisson-Paré D, Ouellet J, Li S, Labrie F, Pelletier G** 2009 Expression of enzymes involved in synthesis and metabolism of estradiol in human breast as studied by immunocytochemistry and in situ hybridization. Histol Histopathol 24:273–282

39. **Haslam SZ** 1988 Local versus systemically mediated effects of estrogen on normal mammary epithelial cell deoxyribonucleic acid synthesis. Endocrinology 122:860–867

40. **Brisken C, O'Malley B** 2010 Hormone action in the mammary gland. Cold Spring Harb Perspect Biol 2:a003178

41. **Bulun SE, Simpson ER** 2008 Aromatase expression in women's cancers. Adv Exp Med Biol 630:112–132

42. **Amin SA, Huang CC, Reierstad S, Lin Z, Arbieva Z, Wiley E, Saborian H, Haynes B, Cotterill H, Dowsett M, Bulun SE** 2006 Paracrine-stimulated gene expression profile favors estradiol production in breast tumors. Mol Cell Endocrinol 253:44–55

43. **Qian L, Lopez V, Seo YA, Kelleher SL** 2009 Prolactin regulates ZNT2 expression through the JAK2/STAT5 signaling pathway in mammary cells. Am J Physiol Cell Physiol 297:C369–C377

44. **Wakao H, Gouilleux F, Groner B** 1994 Mammary gland factor (MGF) is a novel member of the cytokine regulated transcription factor gene family and confers the prolactin response. EMBO J 13:2182–2191

45. **Mouridsen HT** 2006 Incidence and management of side effects associated with aromatase inhibitors in the adjuvant treatment of breast cancer in postmenopausal women. Curr Med Res Opin 22:1609–1621

46. **Khan SI, Zhao J, Khan IA, Walker LA, Dasmahapatra AK** 2011 Potential utility of natural products as regulators of breast cancer-associated aromatase promoters. Reprod Biol Endocrinol 9:91

47. **Simpson ER** 2004 Aromatase: biologic relevance of tissue-specific expression. Semin Reprod Med 22:11–23

48. **Simpson ER, Misso M, Hewitt KN, Hill RA, Boon WC, Jones ME, Kovacic A, Zhou J, Clyne CD** 2005 Estrogen—the good, the bad, and the unexpected. Endocr Rev 26:322–330

49. **Deb S, Zhou J, Jianfeng Z, Amin SA, Imir AG, Gonca IA, Yilmaz MB, Bertran YM, Lin Z, Zihong L, Bulun SE** 2006 A novel role of sodium butyrate in the regulation of cancer-associated aromatase promoters I. 3 and II by disrupting a transcriptional complex in breast adipose fibroblasts. J Biol Chem 281:2585–2597

THE
ENDOCRINE
SOCIETY®

Challenge your diagnostic skills with a one-of-a-kind
self-assessment resource, *Diagnostic Dilemmas: Images in Endocrinology,*
edited by Leonard Wartofsky, M.D.

www.endo-society.org/dilemmas